Journal of Tissue Engineering
Volume 12: 1–19

DOI: 10.1177/20417314209813339
journals.sagepub.com/home/tej
SAGE

Bioengineered *in vitro* skeletal muscles as new tools for muscular dystrophies preclinical studies

Juan M. Fernández-Costa, Xiomara Fernández-Garibay, Ferran Velasco-Mallorquí and Javier Ramón-Azcón

Abstract

Muscular dystrophies are a group of highly disabling disorders that share degenerative muscle weakness and wasting as common symptoms. To date, there is not an effective cure for these diseases. In the last years, bioengineered tissues have emerged as powerful tools for preclinical studies. In this review, we summarize the recent technological advances in skeletal muscle tissue engineering. We identify several ground-breaking techniques to fabricate *in vitro* bioartificial muscles. Accumulating evidence shows that scaffold-based tissue engineering provides topographical cues that enhance the viability and maturation of skeletal muscle. Functional bioartificial muscles have been developed using human myoblasts. These tissues accurately responded to electrical and biological stimulation. Moreover, advanced drug screening tools can be fabricated integrating these tissues in electrical stimulation platforms. However, more work introducing patient-derived cells and integrating these tissues in microdevices is needed to promote the clinical translation of bioengineered skeletal muscle as preclinical tools for muscular dystrophies.

Keywords

Skeletal muscle, tissue engineering, muscular dystrophy, biomaterials, drug screening platforms

Date received: eceived: 30 July 2020; accepted: 26 November 2020

Introduction

Muscular dystrophies (MD) are a group of genetically inherited muscle degenerative disorders characterized by muscle weakness and wasting.[1] The disorders differ in the age of onset, rate of progression, pattern of inheritance, and the type of muscles that are affected (Table 1). Depending on the type of muscular dystrophy, axial, limb, or facial muscles could be affected by a different degree of muscle degeneration and weakness. In specific MDs, other muscles such as cardiac and respiratory are also involved. Moreover, the pathology of some MD disorders has an impact on other organs and tissues as the brain, the skin, the testis, or the eyes. Very rare muscular dystrophies variants are continually identified. To date, more than 50 genes have been determined to be involved in more than 70 inherited muscular dystrophies.[2] These disorders are usually classified into nine main categories or types: myotonic, Duchenne, Becker, Limb-girdle, facioscapulohumeral, congenital, oculopharyngeal, distal, and Emery-Dreifuss.[3] Myotonic syndromes are the most common form in the adult population affecting 1 per 3000 people.[4] In contrast, Duchenne muscular dystrophy is the most prevalent in childhood and is found in roughly 1 per 5000 boys.[5] Although individually muscular dystrophies are considered

Biosensors for Bioengineering, Institute for Bioengineering of Catalonia (IBEC), The Barcelona Institute of Science and Technology (BIST), Barcelona, Spain

Corresponding authors:
Juan M. Fernández-Costa, Biosensors for Bioengineering, Institute for Bioengineering of Catalonia (IBEC), The Barcelona Institute of Science and Technology (BIST), Parc Científic de Barcelona (PCB) Edifici Clúster, c/Baldiri i Reixac, 10-12, Barcelona E08028, Spain.
Email: jfernandez@ibecbarcelona.eu

Javier Ramón-Azcón, Biosensors for Bioengineering. Institute for Bioengineering of Catalonia (IBEC), The Barcelona Institute of Science and Technology (BIST), Parc Científic de Barcelona (PCB) Edifici Clúster, c/Baldiri i Reixac, 10-12, Barcelona E08028, Spain.
Email: jramon@ibecbarcelona.eu

Table 1. Muscular dystrophies classification.

Disease name	Age of onset	Pattern of inheritance (gene affected)	Muscle affected
Duchenne muscular dystrophy (DMD) (OMIM #310200)	Early childhood	XR (DMD; Entrez #1756)	Proximal muscles
Myotonic dystrophies (DM)			
DM1 (OMIM #160900)	Mostly young adulthood, also congenital and childhood-on set	AD (DMPK; Entrez #1760)	Distal muscles
DM2 (OMIM #602668)	Adulthood	AD (CNBP; Entrez #7555)	Proximal muscles
Becker muscular dystrophy (BMD) (OMIM #300376)	Childhood and adulthood	XR (DMD; Entrez #1756)	Proximal muscles
Congenital muscular dystrophies (CMD)			
Bethlem myopathy 1 (BTHLM1) (OMIM #158810)	Congenital	AD (COL6A1; Entrez #1291; COL6A2; Entrez #1292; COL6A3; Entrez #1293)	Proximal muscles
Bethlem myopathy 2 (BTHLM2) (OMIM #616471)	Congenital	AD (COL12A1; Entrez #1303)	Distal muscles
Fukuyama CMD or MD-dystroglycanopathy type A4 (MDDGA4) (OMIM #253800)	Congenital	AR (FKTN; Entrez #2218)	Generalized muscle weakness
MD-dystroglycanopathy type B4 (MDDGB4) (OMIM #613152)	Congenital	AR (FKTN; Entrez #2218)	Generalized muscle weakness
LGMD-dystroglycanopathy type C4 (MDDGC4) (OMIM #611588)	Congenital or early childhood	AR (FKTN; Entrez #2218)	Proximal muscles
CMD with merosin deficiency (MDC1A) (OMIM #607855)	Congenital	AR (LAMA2; Entrez #3908)	Generalized muscle weakness
CMD1B (OMIM #604801)	Congenital	AR (Unknown)	Proximal muscles
CMD1C (OMIM #606612)	Congenital	AR (FKRP; Entrez #79147)	Proximal muscles
CMD1D (OMIM #608840)	Congenital	AR (LARGE1; Entrez #9215)	Generalized muscle weakness
MD-dystroglycanopathy type A1 (MDDGA1) (OMIM #236670)	Congenital-death in the 1st year of life	AR (POMT1; Entrez #10585)	Generalized muscle weakness
MD-dystroglycanopathy type A2 (MDDGA2) (OMIM #613150)	Congenital-death in the 1st year of life	AR (POMT2; Entrez #29954)	Generalized muscle weakness
MD-dystroglycanopathy type A3 (MDDGA3) (OMIM #253080)	Congenital-death in the 1st year of life	AR (POMGNT1; Entrez #55624)	Generalized muscle weakness
MD-dystroglycanopathy type A4 (MDDGA4) (OMIM #253800)	Congenital-death in the 1st year of life	AR (FKTN; Entrez #2218)	Generalized muscle weakness
MD-dystroglycanopathy type A5 (MDDGA5) (OMIM #613153)	Congenital-death in the 1st year of life	AR (FKRP; Entrez #79147)	Generalized muscle weakness
MD-dystroglycanopathy type A6 (MDDGA6) (OMIM #613154)	Congenital-death in the 1st year of life	AR (LARGE1; Entrez #9215)	Generalized muscle weakness
MD-dystroglycanopathy type A7 (MDDGA7) (OMIM #614643)	Congenital-death in the 1st year of life	AR (CRPPA; Entrez #729920)	Generalized muscle weakness
MD-dystroglycanopathy type A8 (MDDGA8) (OMIM #614830)	Congenital-death in the 1st year of life	AR (POMGNT2; Entrez #84892)	Generalized muscle weakness
MD-dystroglycanopathy type A9 (MDDGA9) (OMIM #616538)	Congenital-death in the 1st year of life	AR (DAG1; Entrez #1605)	Generalized muscle weakness
MD-dystroglycanopathy type A10 (MDDGA10) (OMIM #615041)	Congenital-death in the 1st year of life	AR (RXYLT1; Entrez #10329)	Generalized muscle weakness
MD-dystroglycanopathy type A11 (MDDGA11) (OMIM #615181)	Congenital-death in the 1st year of life	AR (B3GALNT2; Entrez #148789)	Generalized muscle weakness
MD-dystroglycanopathy type A12 (MDDGA12) (OMIM #615249)	Congenital-death in the 1st year of life	AR (POMK; Entrez #841897)	Generalized muscle weakness
MD-dystroglycanopathy type A13 (MDDGA13) (OMIM #615287)	Congenital-death in the 1st year of life	AR (B3GALNT1; Entrez #8706)	Generalized muscle weakness
MD-dystroglycanopathy type A14 (MDDGA14) (OMIM #615350)	Congenital-death in the 1st year of life	AR (GMPPB; Entrez #29925)	Generalized muscle weakness
Ullrich CMD type 1 (UCMD1) (OMIM #254090)	Congenital	AD/AR (COL6A1; Entrez #1291; COL6A2; Entrez #1292; COL6A3; Entrez #1293)	Generalized muscle weakness
Ullrich CMD type 2 (UCMD2) (OMIM #616470)	Congenital	AR (COL12A1; Entrez #1303)	Generalized muscle weakness
CMD megaconial type (MDCMC) (OMIM #602541)	Congenital	AR (CHKB; Entrez #1120)	Generalized muscle weakness
Rigid spine muscular dystrophy 1 (RSMD1) (OMIM #602771)	Congenital	AR (SELENON; Entrez #57190)	Proximal limb and facial muscles
CMD due to ITGA7 (OMIM #513204)	Congenital	AR (ITGA7; Entrez #3679)	Proximal muscles
Emery-Dreifuss muscular dystrophy (EDMD)			
EDMD1 (OMIM #310300)	Adulthood	XR (EMD; Entrez #2010)	Calf muscles and upper extremities
EDMD2 (OMIM #181350)	Adulthood	AD (LMNA; Entrez #4000)	Scapuloilioperoneal muscles
EDMD3 (OMIM #616516)	Adulthood	AR (LMNA; Entrez #4000)	Proximal muscles
EDMD4 (OMIM #612998)	Adulthood	AD (SYNE1; Entrez #23345)	Proximal muscles
EDMD5 (OMIM #612999)	Adulthood	AD (SYNE2; Entrez #23224)	Upper limb muscles
EDMD6 (OMIM #300696)	Adulthood	XR (FHL1; Entrez #2273)	Proximal muscles
EDMD7 (OMIM #614302)	Adulthood	AD (TMEM43; Entrez #79188)	Proximal muscles

(Continued)

Table 1. (Continued)

Disease name	Age of onset	Pattern of inheritance (gene affected)	Muscle affected
Facioscapulohumeral muscular dystrophy (FSHD)			
FSHD1 (OMIM #158900)	Adulthood	AD (DUX4; Entrez #100288687)	Facial muscles and upper extremities
FSHD2 (OMIM #158901)	Adulthood	AD (SMCHD1; Entrez #23347)	Facial muscles and upper extremities
Limb-girdle muscular dystrophies (LGMD)			
LGMD1A (OMIM #159000)	Adulthood	AD (MYOT; Entrez #9499)	Proximal muscles
LGMD1C (OMIM #607780)	Childhood and adulthood	AD (CAV3; Entrez #859)	Proximal muscles
LGMD1D (OMIM #603511)	Adulthood	AD (DNAJB6; Entrez #10049)	Proximal muscles
LGMD1E (OMIM #602067)	Adulthood	AD (DES; Entrez #1674)	Proximal muscles
LGMD1F (OMIM #608423)	Young adulthood and adulthood	AD (TNPO3; Entrez #23534)	Proximal muscles
LGMD1G (OMIM #609115)	Adulthood	AD (HNRNPDL; Entrez #9987)	Proximal muscles
LGMD1H (OMIM #613530)	Adulthood	AD (unknwon)	Proximal muscles
LGMD1I (OMIM #618129)	Young adulthood and adulthood	AD (CAPN3; Entrez #825)	Proximal muscles
LGMD2A (OMIM #253600)	Childhood	AR (CAPN3; Entrez #825)	Proximal muscles
LGMD2B (OMIM #253601)	Young adulthood	AR (DYSF; Entrez #8291)	Proximal muscles
LGMD2C (OMIM #253700)	Childhood	AR (SGCG; Entrez #6445)	Proximal muscles
LGMD2D (OMIM #608099)	Childhood	AR (SGCA; Entrez #6442)	Proximal muscles
LGMD2E (OMIM #604286)	Young adulthood	AR (SGCB; Entrez #6443)	Proximal muscles
LGMD2F (OMIM #604287)	Childhood	AR (SGCD; Entrez #6444)	Proximal muscles
LGMD2G (OMIM #601954)	Childhood	AR (TCAP; Entrez #8557)	Proximal muscles
LGMD2H (OMIM #254110)	Childhood	AR (TRIM32; Entrez #22954)	Proximal muscles
LGMD2I (OMIM #607155)	Childhood and adulthood	AR (FKRP; Entrez #79147)	Proximal muscles
LGMD2J (OMIM #608807)	Adulthood	AR (TTN; Entrez #7273)	Proximal muscles
LGMD2K (OMIM #608808)	Childhood	AR (POMT1; Entrez #10585)	Proximal muscles
LGMD2L (OMIM #611307)	Childhood and adulthood	AR (ANO5; Entrez #203859)	Proximal muscles
LGMD2M (OMIM #611588)	Childhood	AR (FKTN; Entrez #2218)	Proximal muscles
LGMD2N (OMIM #613158)	Childhood	AR (POMT2; Entrez #29954)	Proximal muscles
LGMD2O (OMIM #613157)	Childhood	AR (POMGNT1; Entrez #1605)	Proximal muscles
LGMD2P (OMIM #613818)	Childhood	AR (DAG1; Entrez #55624)	Proximal muscles
LGMD2Q (OMIM #613723)	Early childhood	AR (PLEC1; Entrez #5339)	Proximal muscles
Oculopharyngeal muscular dystrophy (OPMD) OMIM(#164300)	Late-onset	AD (PABPN1; Entrez #8106)	Ocular and pharyngeal muscles. Proximal and distal muscles.
Distal muscular myophaties (MPD1)			
MPD1 (OMIM #160500)	Congenital to adulthood	AD (MYH7; Entrez #4625)	Distal muscles
MPD2 (OMIM #606070)	Adulthood	AD (MATR3; Entrez #9782)	Distal muscles with vocal cords weakness
MPD3 (OMIM #610099)	Adulthood	AD (Unknown)	Distal muscles
MPD4 (OMIM #614965)	Adulthood	AD (FLNC; Entrez #2318)	Distal muscles
MPD5 (OMIM #617030)	Young adulthood	AR (ADSS1; Entrez #122622)	Lower limb muscles
MPD6 (OMIM #618655)	Adulthood	AD (ACTN2; Entrez #88)	Lower limb muscles

OMIM = online mendelian inheritance in man; AD = autosomal dominant; AR = autosomal recessive; XR = X-linked recessive; Entrez = entrez molecular sequence database.

rare diseases, the overall prevalence of combined muscular dystrophies was 16.14 per 100,000,[6] and therefore, they have a great impact on society.

Palliative treatments are availed for these diseases, although there is no cure for any muscular dystrophy to date. Remarkably, in the last decade, some drugs for specific muscular disorders have been developed, including small molecules and antisense oligonucleotides.[7–11] However, these treatments must demonstrate efficacy and safety in the clinical phases before being widely used in patients. The development of a new drug takes years, even decades, from preclinical studies to reach the market and it is a very costly process.[12] Drug development implies three main stages: discovery, preclinical studies, and clinical trials. During the preclinical stage, extensive studies with *in vitro* and animal models provide preliminary information on the efficacy, toxicity, pharmacokinetics, and safety of a drug candidate. However, the probability of success of a molecule after entering the clinical phases is only 10%.[13] This low success rate is mostly due to the high toxicity or low efficacy of the drug in humans. This suggests that current preclinical models should be improved to reduce costs and accelerate drug development time. Furthermore, the heterogeneity of muscular dystrophy manifestations anticipates that each patient would respond to treatments differently. Therefore, there is also a clinical need for personalized therapies to target these diseases effectively. Human bioengineered *in vitro* tissues are emerging as new tools for preclinical research.[14,15] Specifically, bioengineered *in vitro* skeletal muscles would provide more efficient and predictive models to improve drug development for muscular dystrophies. Here, we discuss the recent advances in skeletal muscle tissue engineering, focusing on new human in vitro models for muscle analyses and their application in the study of muscular dystrophies. This review was designed with two main purposes: to bring the clinician community closer to the bioengineering technologies for skeletal muscle and to show a general overview of the complexity of muscular dystrophies to researchers working on skeletal muscles tissue engineering.

Skeletal muscle structure and myogenesis regulation

Skeletal muscle is the largest tissue in the body, accounting for almost 40% of body mass.[16] Skeletal muscle architecture is characterized by a very particular and well-described arrangement of muscle fibers, also called myofibers. Groups of myofibers form the fascicles, and bundles of fascicles make up the whole muscle tissue (Figure 1). Myofibers are formed by the fusion of myoblasts to produce multinucleated myotubes, which mature further in myofibers.[17] The dimensions of a single myofiber are approximately 100 μm in diameter and 1 cm in length, and its nuclei are located along the periphery of the whole fiber. The mature skeletal myofiber contains a highly organized cytoskeleton made up of aligned myofibrils, which are repeating consecutive sections of the functional unit of skeletal muscle, the sarcomere.[18] Sarcomere complex structure is composed of two main alternating sets of protein filaments: thin filaments (α-actin and associated proteins) and thick filaments (myosin and associated proteins), which run parallel to the muscle fiber axis. At a molecular level, the sarcomeric contraction consists of the movement of the myosin heads on actin filaments. Thus, the formation of correctly aligned myofibrils is fundamental for muscle function. So, to engineer skeletal muscle *in vitro*, its complex anatomy structure must be mimicked using biomaterial scaffolds and specific biofabrication techniques.

Muscle development and regeneration are regulated by a hierarchy of myogenic regulatory factor (MRF) family of transcription factors[19] (Figure 2). Stem cells in the muscle are called satellite stem cells (SSCs) and are produced by activation of precursor cells expressing PAX3 and PAX7.[20,21] The expression of MYF5 and MYOD1 in SSCs induces the myogenic program to produce myoblasts. Myogenesis process continues with the activation of MYOG and MEF2 and the downregulation of MYF5 and MYOD1. Activation of a second wave of MRFs (MYOG and MRF4) induces terminal differentiation of myoblasts into myotubes. Mature myotubes additionally express muscle-specific genes such as the contractile proteins of the muscle as myosin heavy chain (MHC), actin, titin, among others, and a reduction in expression of MYOG.[22]

The skeletal muscle extracellular matrix

As mentioned above, the formation of aligned myofibers is an essential factor for skeletal muscle tissue engineering. Nonetheless, it is important to consider that *in vivo*, these fibers are embedded within a 3D scaffold, the skeletal muscle extracellular matrix (ECM), mainly composed of collagens, non-collagenous glycoproteins, proteoglycans, and elastin.[23] Besides being a scaffold for cell-matrix interactions, the skeletal muscle ECM plays a crucial role in skeletal muscle function. For instance, it allows a uniform distribution and transmission of force within muscle and from muscle to tendon. Furthermore, the ECM interactions are critical to maintaining the mechanical homeostasis within the muscle.[18]

The skeletal muscle ECM is traditionally classified into three organized layers: endomysium, perimysium, and epimysium (Figure 1). The endomysium (also called basement membrane) surrounds individual myofibers. The perimysium is a thickened ECM that encapsulates the fascicles, and the epimysium is a dense layer that

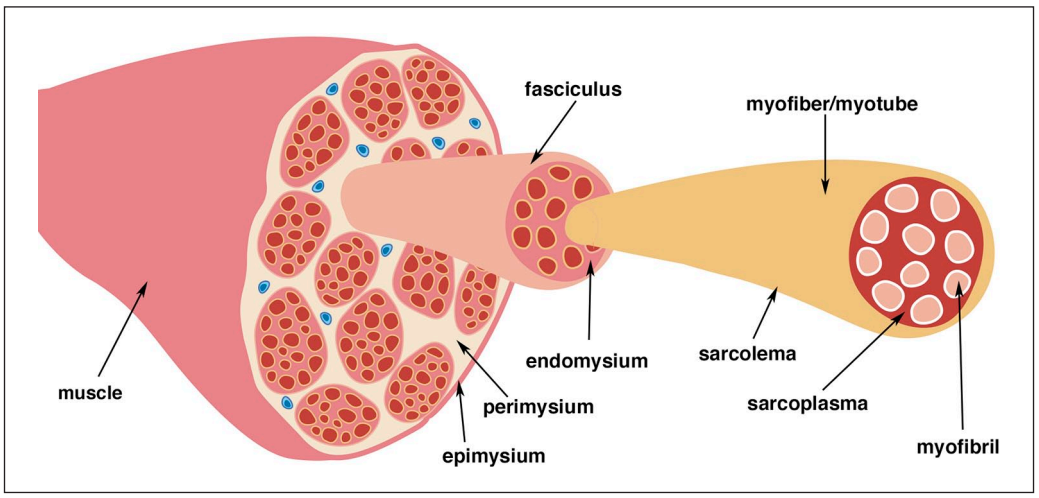

Figure 1. Structure of muscle anatomy. Epimysium covers each muscle. Muscle fibers are grouped forming bundles (fascicles). Each fasciculus is surrounded by perimysium while endomysium surrounds the myofibers. Each individual myofiber or myotube have a membrane (sarcolemma) and is composed of hundreds of myofibrils. Myofibrils are the functional contractile unit of the muscle and are surrounded by sarcoplasm.

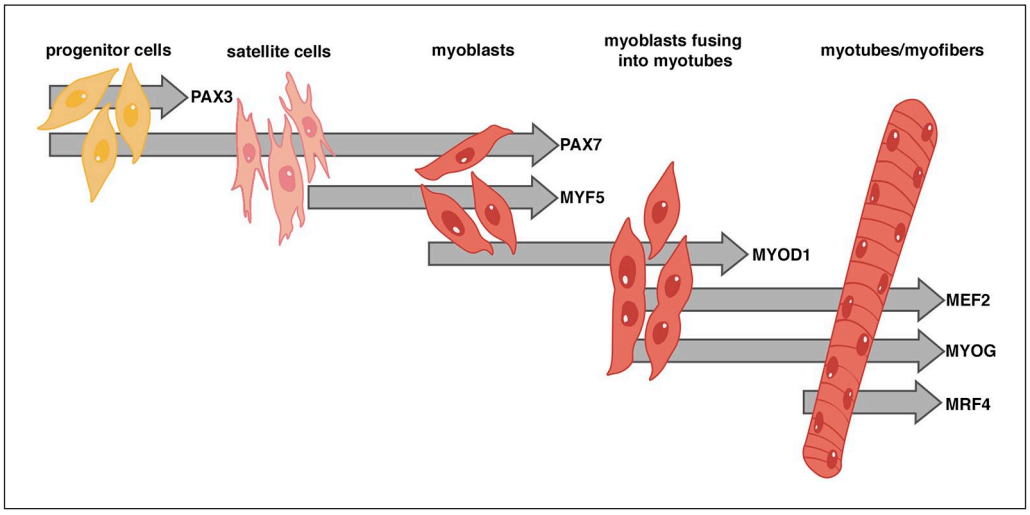

Figure 2. Regulation of myogenic differentiation by a hierarchy of transcription factors. Satellite cells expressing PAX7 derive from the PAX3/PAX7 expressing progenitor cells. Following activation of MYF5 expression in satellite myogenic cells, the myogenic program starts, and MYOD1 expression is activated. Activation of MYOG and MEF2, with downregulation of MYF5 and later MYOD1, marks the start of terminal differentiation into myofibers. Activation of MRF4 happens several days after the induction of differentiation, following a reduction in MYOG expression.

surrounds the whole muscle. However, as the knowledge about the ECM roles and complexity increases, it has been argued that a less simplistic ECM organization should be established.[18,23,24]

Among the skeletal muscle ECM proteins, collagens are the most abundant, glycoproteins are involved in tissue organization and cell-matrix interactions, and proteoglycans are involved in signaling and tissue regeneration.[18] The basement membrane consists mainly of collagen type IV and laminins, whereas collagen type I is found mostly in the peri- and epimysium. Together all types of collagens provide structural support and allow tissue mechanotransduction.[25] Briefly, fibrillar collagen type I provides tensile strength and rigidity, while collagen type III fibers form a loose mesh that gives elasticity to the inner layers of the intramuscular connective tissue. Moreover, collagen type IV integrates laminins and other proteins into a stable structure. In less abundance, collagen type VI is present in all ECM layers.[23] Interestingly, collagen type VI mutations cause disorders involving both muscle and connective tissue, such as congenital muscular dystrophies as Ullrich CMD type 1 (UCMD1) and Bethlem Myopathy type 1 (BTHLM1) (see Table 1).[26]

Engineering topographical cues for skeletal muscle 2D culture

Skeletal muscle represents a complex and challenging tissue for *in vitro* generation through tissue engineering. Given the importance of the aligned structure of myofibers for their correct functionality, the main fabrication strategies are focused on providing geometric cues (Table 2). The most recent published approaches to culture myofibers on aligned structures can be classified into three main types: micropatterning, electrospinning, and bioprinting.

Micropatterning

The simplest models for generating skeletal muscle *in vitro* are based on the 2D culture of myoblasts seeded on micromolded substrates. RNAseq analyses of C2C12 murine myotubes on micropatterned gelatin hydrogels showed that cells display an increased ability to form aligned sarcomeres and increased contractile protein expression, demonstrating the effect of topographic cues in the maturation of muscle cells.[27] Another technique to generate 2D micropatterned scaffolds is microcontact printing. For example, Vajanthri and collaborators used the microchanneled flowed plasma process to generate different cell adhesive micropattern coated glass with 3-amino-Propyltriethoxysilane (APTES) and Octadecyltrichlorosilane (OTS).[28] Aligned myotubes grew onto stamped micropatterned regions. Micropatterned substrates also emerged as great potential substrates to align and differentiate myoblasts.[29] In this study, the authors generated a new platform by crumpling graphene uniaxially (Figure 3(a)). Micropattern dimensions were modulated by applying compressing strain. Culture of C2C12 mouse myoblast on this uniaxially crumpled graphene promoted the alignment and elongation at a single-cell level and enhanced differentiation and maturation of myotubes. Other graphene-based approaches used femtosecond laser ablation to generate a patterned substrate in polyacrylamide hydrogels.[30] Studying different pattern distances, the authors concluded that 50 μm of spacing produced the better alignment and maturation of myotubes. Myogenic differentiation could also be improved by applying electrical stimulation to these micropatterned cultures. An alternative approximation used poly(ethylene glycol) (PEG)-based microgrooved hydrogels to provide topographical and electrical stimuli to cells.[31] To enhance hydrogel electrical properties and cell attachment, poly(3,4-ethylenedioxythiophene) (PEDOT) and tripeptide Arg-Gly-Asp (RGD) were combined with the PEG-hydrogel.

Electrospinning

One of the most common techniques for 2D cell guidance and tissue engineering is electrospinning.[32] Electrospinning technique has been successfully used to generate mature myotubes over microfibres fibrin bundles.[33] Mechanical strains were applied to enhance the myogenic differentiation of the immature myoblasts. In this study, several strain cycles were tested, and delayed strain onset improved or maintained myogenic outcomes. Electrospinning technique has also been used to co-culture C2C12 murine myoblasts and human umbilical vein endothelial cells (HUVEC).[34] To guide the cells and promote their fusion, the authors used Polyvinyl alcohol (PVA)-leached polycaprolactone (PCL) and collagen struts as mechanical supporters with topographical cues. HUVECs-laden alginate bioink was uniaxially electrospun on these supporters. C2C12 myoblasts seeded on this vascularized scaffold formed mature myofibers with striated myosin heavy chain (MHC) protein patterns. Recently, poly (vinylidene fluoride) (PVDF) was used as an electroactive biomaterial to enhance the myoblasts fusion and myogenic maturation due to its piezoelectric properties.[35] A piezoelectric material becomes electrically polarized upon a mechanical stimulation.[36] This propriety can be used to give an electrical signal to the cells. In this work, C2C12 cells were seeded on an electrospun aligned matrix of PVDF. Charged surfaces improved the fusion of muscle cells into differentiated myotubes.

Bioprinting

Similar to electrospinning, bioprinting and other 3D-based approaches have been widely used to generate highly aligned fibers.[37–42] E-field printing, a combination of e-field and 3D printing, was used to engineer PCL highly hierarchical scaffolds.[37] The growth of C2C12 myotubes on top of these scaffolds enhanced cell alignment and increased myogenic markers. Another technique to promote myotubes alignment is culturing them on bioprinted gelatin methacryloyl (GelMA) over a thermoresponsive poly(N-isopropylacrylamide) (PNIPAm) coated substrate.[38] After seeding cells, the temperature was lowered to detach cells from PNIPAm surfaces. With this approximation, directed collective cell migration was regulated (Figure 3(b)). Similarly, microfluidic spun GelMA fibers with have a well-defined surface morphology have been generated by extrusion through a microgrooved mold (Figure 3(c)).[39,40] Topographical cues on micropatterned GelMA fibers promoted alignment of C2C12 myoblasts and myotube formation. The combination of topographical cues with agrin treatment further enhanced myotube maturation and functionality, as shown by improved contractility under electrical stimulation.[40] Extrusion of collagen fibers has also been used as geometrical cues to fabricate endothelialized and aligned skeletal muscle.[41,42] Co-culture murine myoblasts with endothelial cells on nano-fibrillar collagen scaffold strips promotes the formation of highly organized myofibers and microvasculature (Figure 3(d)). Remarkably, the implantation of these scaffolds in injured mice muscle favored vascular regeneration as a promising

Table 2. Novel bioengineering approaches to fabricate skeletal muscle models.

Biomaterial	Cellular type	Biofabrication technique	Highlights	Reference
Alginate—PEO bioink with PLC	C2C12 myoblasts and HUVEC endothelial cells	3D printing and electrospinning	Biophysical and biochemical cues facilitate myoblast alignment	Yeo and Kim[34]
Alginate—pluronic PF127	C2C12 myoblasts	3D bioprinting	High-throughput fabrication of small muscle bundles	Mozetic et al.[52]
Collagen	C2C12 myoblasts and Human microvascular endothelial cells	Extrusion technique	Implantation of endothelialized skeletal muscle tissue enhances microvascularization	Nakayama et al.[41]
Collagen	C2C12 myoblasts	Micromolding	Development of a 3D myogenesis approach with a vessel embedded system	Wan et al.[58]
Collagen with gold nanowires	C2C12 myoblasts	3D bioprinting	New bioink with gold nanowires as cell aligners that improve the cell orientation when applying an electrical field	Kim et al.[49]
Collagen—Matrigel®	Primary myoblasts from mdx mouse model	3D casting	Automated drug screening BAM-based platform	Vandenburgh et al.[38]
Collagen—Matrigel®	Primary human myoblasts	3D casting	High throughput micro-muscle platform.	Mills et al.[76]
dECM	C2C12 myoblasts	Thermal gelation	New biomaterial that enhances muscle regeneration when transplanted	Lee et al.[65]
dECM	Primary human myoblasts and HUVEC endothelial cells	3D bioprinting	Enhanced muscle regeneration after implantation of prevascularized muscle bundles in a rodent model	Choi et al.[83]
dECM—MA	C2C12 myoblasts	3D bioprinting	Development of a biochemical and topographical cued biomaterial scaffold	Kim et al.[37]
Fibrin	Human primary muscle progenitor cells (hMPCs)	3D bioprinting	Functional recovery after implantation of multilayered bundles in a rodent model	Kim et al.[81]
Fibrin	Primary human myoblasts	3D casting	Intramuscular drug delivery in vitro model	Gholobova et al.[82]
Fibrin	iPSCs from DMD, LGMD other CDM patients	3D casting	Mature myotube recapitulates pathogenic hallmarks	Maffioletti et al.[92]
Fibrin	C2C12 myoblasts	Electrospinning	Study of different mechanical strains to improve myogenic outcomes	Somers et al.[33]
Fibrin	C2C12 myoblasts	Micromolding	Fabrication of a high-throuput multiassay platform for the generation of engineered contractile muscle bundles	Christensen et al.[59]
Fibrin—Gelatin	C2C12 myoblasts	3D bioprinting	Study of force modulation and adaptability of 3D printed muscles	Mestre et al.[49]
Fibrin—Geltrex®	Primary human myoblasts and human stem cells-derived motoneurons	Hydrogel molding of bundles attached to Velcro® anchors	Myobundles with neuromuscular junctions in long-lasting cultures	Bakooshli et al.[80]
Fibrin—Matrigel®	Primary human myoblasts	Hydrogel molding of bundles within nylon frame	First functional engineered skeletal muscle	Madden et al.[77]
Fibrin—Matrigel®	Human induced pluripotent stem cells	Hydrogel molding of bundles within nylon frame	First functional engineered human skeletal muscle from induced pluripotent stem cells	Rao et al.[78]
Fibrin—Matrigel®	Primary human myoblasts	Hydrogel molding of bundles within nylon frame	Engineered myobundles with the highest specific forces reported to date	Khodabukus et al.[79]
Gelatin	C2C12 myoblasts	Micropatterning	Enhancing of the expression sarcomeric genes	Denes et al.[27]
Gelatin—CMC	C2C12 myoblasts	Cryogelation	New volumetric and conductive anisotropic scaffold that allows microscale constructs	Velasco-Mallorquí et al.[61]
GelMA	C2C12 myoblasts	Microfluidic extrusion device	Patterned surface fibers enhance myogenic differentiation	Shi et al.[39] and Ebrahimi et al.[40]
GelMA	C2C12 myoblasts	3D casting	Characterization of geometrical confinement and mechanical stiffness of scaffolds	Costantini et al.[55]
GelMA—Alginate	C2C12 myoblasts	3D bioprinting	New biomaterial with oxygen-generating source	Seyedmahmoud et al.[44]

(Continued)

Table 2. (Continued)

Biomaterial	Cellular type	Biofabrication technique	Highlights	Reference
GelMA and collagen methacrylate	C2C12 myoblasts,human adipose stem cells and human primary muscle progenitor cells (hMPCs)	3D bioprinting	Functional GelMA-based bioink for highly aligned scaffolding	Kim and Kim[48]
GelMA on poly(N-isopropylacrylamide) (PNIPAm)	C2C12 myoblasts	Printing	New method to study the regulation of cell migration	Du et al.[38]
GelMA, CMCMA—GelMA, AlgMA—GelMA and PEGDA—GelMA	C2C12 myoblasts	3D Bioprinting	Characterization of different GelMA composite biomaterials for skeletal muscle tissue engineering	García-Lizarribar et al.[50]
GelMA—Alginate	C2C12 myoblasts	3D Bioprinting	A new method to induce macroscale cell alignment with multi-layered scaffolds	Lee and Yeong[65]
GelMA—CMCMA	C2C12 myoblasts	Micromolding	Integration of skeletal muscle tissue with microfluidic sensing platform	Ortega et al.[56]
Graphene	C2C12 myoblasts	Micropatterning	New graphene 2D platform that enhances cell alignment and differentiation	Kim et al.[49]
Graphene oxide—polyacrylamide	C2C12 myoblasts	Micropatterning	Development of a conductive multifunctional biomaterial that enhances myogenic maturation by applying electrical pulse stimulation	Park et al.[30]
Laminin, fibrin, or Matrigel®	Primary myoblasts from DMD patient	2D micropatterning	Myotubes with DMD pathological hallmarks	Serena et al.[91]
OTS and APTES	C2C12 myoblasts	Micropatterning	New method of micropatterning to obtain aligned muscle cultures	Vajanthri et al.[28]
Oxidized alginate—Gelatin	C2C12 myoblasts	3D Bioprinting	Easy method to align cells by combining bioprinting with appropriate shear stress	Distler et al.[47]
PEG—Fibrin	C2C12 myoblasts	3D bioprinting	Novel approach to generate skeletal muscle using a self-made 3D bioprinting	Costantini et al.[51]
Poly lactic-co-glycolic acid (PLGA)	C2C12 myoblasts	E-jet 3D printing	3D printed platform with 50 µm fibrillar gap enhances cell adhesion and proliferation	Chen et al.[53]
Poly(ethylene glycol) (PEG)—poly(3,4-ethylenedioxythiophene) (PEDOT)	C2C12 myoblasts	Micropatterning	Fabrication of a conductive microgrooved hydrogel for myogenic differentiation	Gong et al.[31]
Poly(lactic-co-glycolic acid) (PLGA)	C2C12 myoblasts	Microfluidic droplet emulsion	Generation of a porous spheres microcarriers for cell delivery	Kankala et al.[14,62]
Poly(vinylidene fluoride) (PVDF)	C2C12 myoblasts	Electrospinning	Piezoelectric scaffold enhances in vitro muscle regeneration	Ribeiro et al.[35]
Polycaprolactone (PCL)	C2C12 myoblasts	E-field assisted 3D printing	New technique to generate highly aligned skeletal muscle tissue	Kim et al.[37]

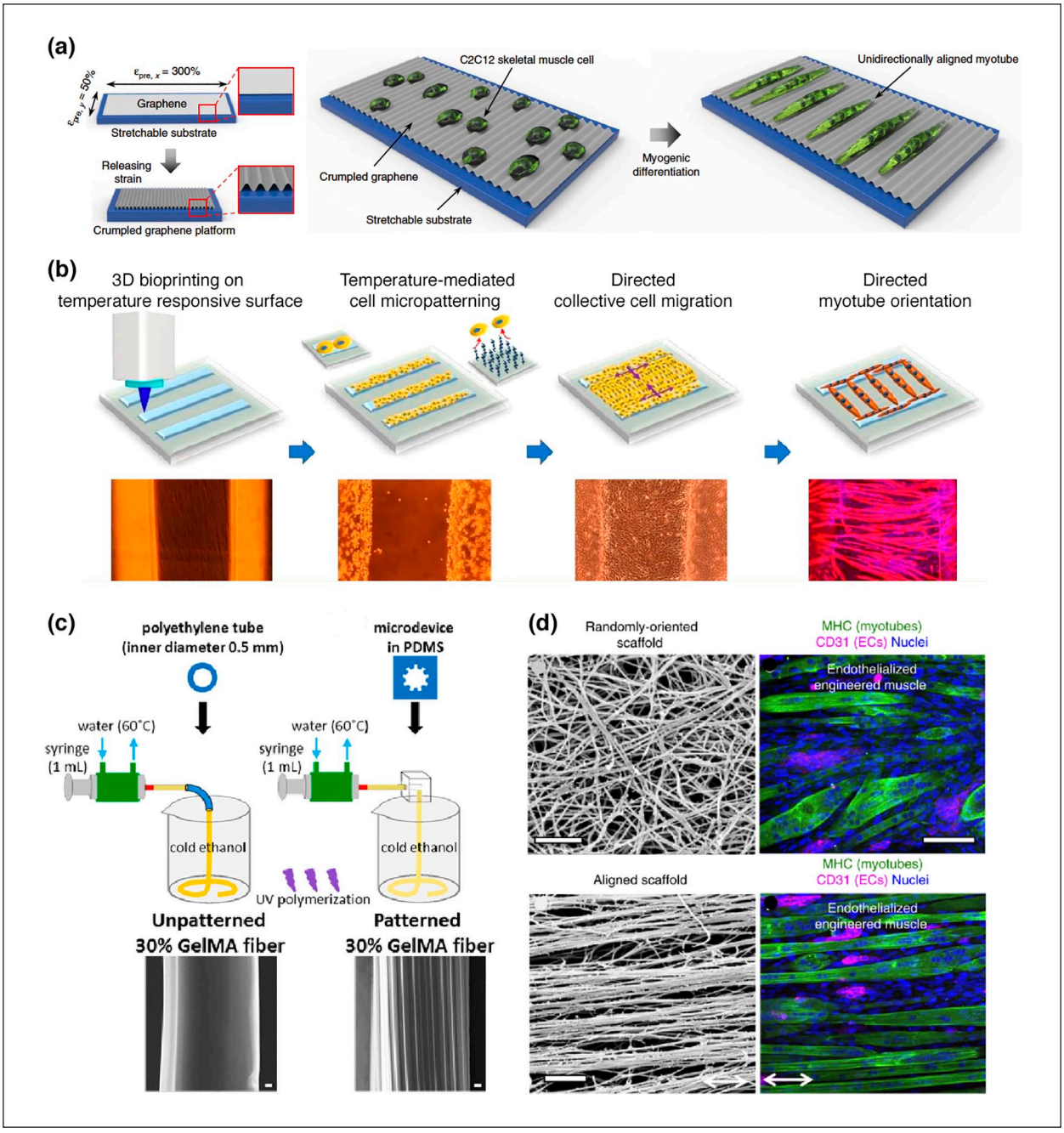

Figure 3. Engineering topographical cues for the 2D culture of skeletal muscle. (a) Fabrication of an anisotropically crumpled graphene platform by releasing the elastomeric substrate on which a graphene film was attached. C2C12 cells were cultured on top of these substrates to differentiate and align C2C12 cells on crumpled graphene. Adapted from Kim et al.[29]. (b) Gelatin methacryloyl (GelMA) hydrogel micropatterns were 3D printed on a thermo-responsive polymer (poly(N-isopropylacrylamide), PNIPAm). Temperature control was used to promote directed collective C2C12 cell migration on the GelMA patterns to induce myotube formation and orientation. Adapted with permission from Du et al.[38]. Copyright 2019 American Chemical Society. (c) Schematic representation of the fabrication process of unpatterned and micropatterned GelMA fibers. Field emission-scanning electron microscope images showing surface structures of the GelMA fibers. Scale bars: 20 μm. Adapted with permission from Ebrahimi et al.[40]. (d) Characterization of endothelialized engineered murine muscle. Scanning electron microscopy images of randomly oriented or aligned scaffold nanofibers. Confocal microscopy images showing myosin heavy chain (MHC, green) and CD31 (magenta) staining in differentiated myotubes in randomly oriented or aligned scaffolds. Adapted from Nakayama et al.[41]. The images in panel (c) are not published under the terms of the CC-BY license of this article. For permission to reuse, please see Ebrahimi et al.[40].

treatment of volumetric muscle loss.[41] In summary, the results obtained by micropatterning, electrospinning, and bioprinting approaches confirm that the geometrical cues are fundamental for engineering mature myotubes *in vitro*.

3D Engineering for skeletal muscle culture

Bioengineering approaches in 2D models have been useful to study biomaterials and the importance of the topological cues for in vitro culture of skeletal muscle tissue. However, these techniques do not resemble the environment of the native skeletal muscle. For this reason, three-dimensional scaffolds have become the gold standard to generate skeletal muscle tissue. In order to mimic the extracellular environment and the native cellular morphology, the main bioengineering strategy is focused on the 3D encapsulation of muscular cell precursors in biocompatible materials. In the last years, 3D bioprinting,[43–54] hydrogel molding,[55–59] and microporous scaffolds[60–62] have been implemented to fabricate skeletal muscle tissues.

3D Bioprinting

Several biomaterials can be used as bioinks to print encapsulated myoblasts in various 3D structures to obtain aligned myotubes. Among these, GelMA and other methacrylated polymers are the most used biomaterials in bioprinting due to is photocrosslinkable properties. 3D bioprinting was used to fabricate tissue constructs using GelMA with alginate and C2C12 cells.[44] Interestingly, the metabolic activity of myotubes was improved by adding calcium peroxide, an oxygen-generating particle, to the bioink. Oxidized alginate has also been used in combination with gelatin as a bioink. The cells orientate with the proper nozzle size and extrusion pressure due to the shear stress during the bioprinting process.[47] The cells grow in the direction of printing, migrate to the hydrogel surface over time, and differentiate into aligned myotubes. 3D printed GelMA-alginate hydrogels with Plurionic F-127 as a sacrificial layer were used to induce a macroscale level of controlled cell alignment with angle variation. The variation in the grid pattern angles was designed to mimic the fibril orientation of native tissues, where angles of cell alignment vary across the different layers. In a similar approach, GelMA and collagen methacrylate were bioprinted and UV crosslinked to generate different 3D structures and obtain mature aligned myotubes.[48] To better control the cell alignment, cell aligners could be added to the bioinks. One way to achieve this was by printing collagen with gold nanowires and applying a field into this extruded biomaterial. These gold nanowires were aligned following the desired directionality by applying an electric field. The use of gold nanowires enhanced myoblast alignment inside the hydrogel by contact guidance.[49] Moreover, the addition of gold nanowires improves the electrical properties of the scaffolds. These works used bioinks based on natural polymers as gelatin or collagen due to their biocompatibility. However, these materials are degradable by mammalian cells, causing a loss of the hydrogel structure, limiting long-term cell cultures. To overcome this, materials that are non-degradable by mammalian cells have been combined with these natural polymers to improve the mechanical properties of the scaffolds. C2C12 cells were encapsulated in different combinations of GelMA-based composite bioinks.[50] A structure of hydrogel filaments was bioprinted with these bioinks (Figure 4(a)). The combination of GelMA with methacrylated carboxymethylcellulose (CMCMA) resulted in the most suitable properties for skeletal muscle tissue engineering. Remarkably, the GelMA-CMCMA composite biomaterial has been used for the long-term culture of C2C12 myotubes. The 3D structure of the hydrogel remained in time for 3 weeks, enhancing myotube maturation.[57] Alternative combinations of natural and synthetic biomaterials are suitable for bioprinting skeletal muscle cells. Aligned myoblast-laden hydrogels of PEG-fibrinogen have been produced using microfluidic-enhanced 3D bioprinting.[51] Moreover, Pluronic/alginate blends have been investigated as a model system for culture of C2C12 murine myoblast.[52] Fabricated constructs exhibited high cell viability, as well as a significantly improved expression of myogenic markers. To mimic the extracellular matrix, poly lactic-co-glycolic acid (PLGA) multilayered scaffolds were made with E-jet 3D printing.[53] By comparing different fibrilar gaps in the scaffolds, the authors concluded that 50 μm gaps enhance cell adhesion and proliferation. In all the previous works, the bioprinting design was based on lines or meshes to guide the alignment of myotubes. Alternatively, hydrogels can be printed to compact around post structures and generate skeletal muscle tissue.[45,46,54] These kinds of platforms allow the force measurement of skeletal muscle after electrical stimulation. Skeletal muscle tissue contractions cause the bending of the pillar. This displacement is used as a proportional measurement of the muscle bundle forces.

Micromolding

To generate aligned scaffolds, an alternative technique to bioprinting is hydrogel micromolding. Molds of polydimethylsiloxane (PDMS), a biocompatible transparent polymer, are the most used to transfer aligned micropatterns to the 3D hydrogels.[63,64] Optimal stiffness of hydrogels for skeletal muscle bioengineering was determined by changing GelMA concentration and UV crosslinking time. Using molds with channels of different widths, the authors investigated the effect of geometrical confinement and hydrogel stiffness for C2C12 myotube culture.[55] The best results were obtained with the thinnest 0.5 mm channels and a low stiffness between 1 to 3 kPa. Murine skeletal muscle tissue

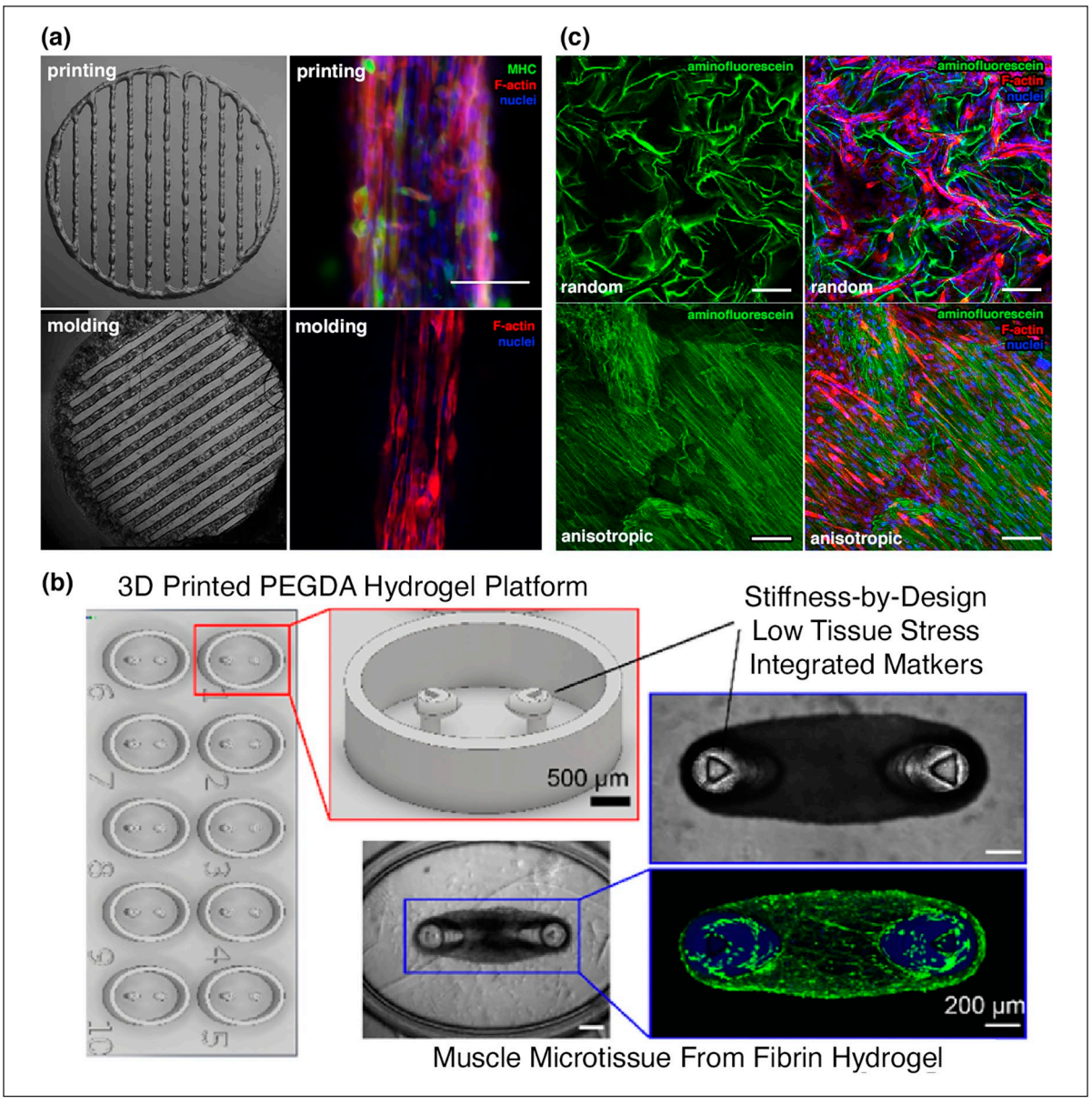

Figure 4. Engineering strategies for the 3D culture of skeletal muscle tissue. (a) C2C12 myotubes formation in bioprinted or molded composite hydrogels. Top view images of the composite hydrogels after fabrication. Confocal microscopy showing F-actin in red, MHC in green, and nuclei in blue. Scale bar: 200 µm. Adapted with permission from Garcia-Lizarribar et al.[50] and authors unpublished results. (b) Multi-assay 3D printed poly(ethylene glycol) diacrylate (PEGDA) hydrogel platforms for casting fibrin hydrogel muscle bundles. Adapted with permission from Christensen et al.[59]. Copyright 2020 American Chemical Society. (c) Confocal microscopy images showing aminofluorescein-marked cryogels in green, cells marked with phalloidin in red and cell nuclei counterstained in blue with DAPI. Scale bars: 100 µm. Adapted from Velasco-Mallorqui et al.[61]. The images in panel (a) are not published under the terms of the CC-BY license of this article. For permission to reuse, please see Garcia-Lizarribar et al.[50].

has also been generated by micromolding of GelMA-CMCMA hydrogels.[56,57] Here, C2C12 cells were encapsulated by photomold patterning of the hydrogel using a microgrooved PDMS stamp (Figure 4(a)). Interestingly, these tissues were implemented in cytokine sensing platforms to analyze responses to biological and electrical stimuli. Micromolding and micromilling techniques were combined with posts to develop a new organ-on-a-chip set up with a vessel embedded system.[58] To vascularize the engineered muscle bundle, C2C12 and HUVEC were co-cultured by using collagen and a sacrificial layer and supported by pillars. To mass-produce structures with posts or cantilevers, Christensen et al. described a stereolithographic method to 3D print poly(ethylene glycol) diacrylate (PEGDA) hydrogels with high precision and high accuracy (Figure 4(b)).[59] These PEGDA platforms with

anchored cantilevers were used to cast fibrin hydrogel muscle bundles around these pillars.

Extracellular matrix derived materials obtained by decellularization (dECM) have emerged as novel natural hydrogels to engineer muscle tissue.[65,66] These dECM-derived hydrogels contain growth factors, cytokines, proteoglycans, and structural adhesive proteins, which represent tissue-specific biochemical cues.[67] Murine skeletal muscle generated with dECM scaffolds present more mature myotubes than with collagen scaffolds.[65] Moreover, a significantly greater number of myofibers were observed when compared to collagen scaffolds after implantation of both engineered skeletal tissues in a rabbit tibialis anterior (TA) muscle defect model. Going a step further, methacrylation of dEMC allows bioprinting and photocrosslinking of the hydrogels, providing topological cues for skeletal muscle engineering.[66]

Microporous scaffolds

An alternative fabrication method that allows the generation of millimeter range scaffolds is cryogelation.[60] Cryogels are microporous scaffolds with a pore range from a few micrometers up to hundreds of micrometers.[68] After freezing the polymer solution, ice crystals are formed. Once the cryogel is thawed, the ice crystals leave behind empty pores. The pore morphology can be modulated by applying different freezing directionalities.[69,70] Highly aligned morphology is a necessary geometrical cue for skeletal muscle maturation. For this reason, anisotropic gelatin-cellulose cryogels were generated to engineer volumetric skeletal muscle using C2C12 myoblasts.[61] Anisotropic cryogels improve cell alignment, myotube fusion, and myogenic maturation (Figure 4(c)). Moreover, the addition of carbon nanotubes (CNTs) to the cryogel improves the electrical properties of the scaffolds, which enhances early myogenic maturation steps when electric pulse stimulation is applied. Interestingly, these gelatin-cellulose cryogels are easy to handle without affecting their shape. Therefore, this technique has strong possibilities for tissue engineering and organ-on-a-chip technologies.

Microporous scaffolds can also be used for skeletal muscle cell delivery by generating highly open porous microspheres (HOMPs).[62] These microspheres were fabricated of biocompatible PLGA by microfluidic droplet emulsion. These HOPMs with interconnected pores facilitated a high cell adhesion rate, continuous proliferation, and augmented myogenic differentiation of C2C12 after transplantation in mouse muscle.

Computational modeling

Despite the promising potential of all these approaches to generate 3D muscle tissues *in vitro*, there are still many technical limitations. To complement the lack of chemical or mechanical information of many experimental models, computational modeling has gained a relevant role. Using computational methodologies as agent-based model (ABM) for individual cell modeling, or finite element method (FEM) for cellular population density, it is possible to study the cell behavior inside scaffolds and between cells. As a clear example of this combination between technical and computational methods, Torri et al.[71] used the data from the previous work from Smith et al.[72] to analyze the muscle cell behavior *in silico*. They applied both modeling approaches with successful results achieving a good resemblance between their approximations *in silico* and the *in vitro* studies. These analyses point to the potential of computational modeling to predict uncertain variables and complement *in vitro* experiments.

Functional human skeletal muscle tissue models

In the last decade, skeletal muscle bioengineering techniques have been developed using mainly murine myoblasts as a cell model. These studies shed light on important features for skeletal muscle tissue engineering, such as topological cues, biomaterials, and biochemical factors. The next step in skeletal muscle bioengineering is incorporating human cells to obtain more relevant models for muscular dystrophies. Human skeletal muscle tissue models have been developed from primary and immortalized human myoblasts and human induced pluripotent stem cells (hiPSCs) [reviewed in[73]]. It has recently been shown that human amniotic mesenchymal stem cells (hAMCs) can undergo myogenic differentiation. Moreover, hAMCs express key growth factors that promote endothelial cell proliferation and angiogenesis, representing a great advantage as a cell source for skeletal muscle tissue engineering.[74]

In general, human myogenic precursor cells are encapsulated in hydrogel scaffolds that aim to mimic the 3D environment of native muscle tissues. The most common hydrogels are those of natural origin, especially collagen,[75,76] fibrin,[77–82] and dECM.[83] The main fabrication strategies have been hydrogel molding[75–80] or 3D printing[81–83] (Table 2). In this way, cell alignment is achieved through passive tension, allowing long-term cell culture, and enhancing muscle maturation and function. The first 3D skeletal muscle tissues reported consisted of myoblasts encapsulation in a collagen I matrix that contracts around pillars.[84,85] The contraction of the matrix promotes cell alignment in the direction of the anchoring points, producing long multinucleated myofibers.[75] Collagen I is one of the main components of the skeletal muscle extracellular matrix.[23] However, it has been observed that myogenic maturation and contractile force of the tissue can be compromised by the relatively high stiffness of the collagen hydrogel, especially for large macroscopic constructs.[25,86] For this reason, in the last years, efforts have been directed

to incorporate materials with better mechanical properties. Fibrin composite hydrogels have resulted in the most promising materials to generate functional skeletal muscle constructs due to their ability to be remodeled by cells and induce ECM synthesis.[87]

Functional human skeletal muscle tissues or bioartificial muscles (BAMs) were developed for the first time in the Bursac lab using primary human myoblasts. By molding fibrin-Matrigel® hydrogels within PDMS molds inside a nylon frame, the authors created muscle 3D bundles[77] (Figure 5(a)). In this platform, active force measurements were performed in response to electrical and biological stimulation. In 2018, following the same biofabrication approach, the authors reported the generation of skeletal muscle tissues derived from direct reprogramming of hiPSCs.[78] Overexpression of PAX7 was induced to generate satellite cell-like cells. Remarkably, human muscle 3D bundles were kept in culture for up to 4 weeks, being the longest culture time reported to the date. Of note, muscle constructs presented a correct membrane localization of dystrophin and generated active twitch and tetanic contractions. Interestingly, after 4 weeks of culture, these tissues retained a pool of PAX7+ cells together with MYOG+ myotubes, mimicking the satellite-cells presence in native muscle. Although these models present different myotube maturation levels, it has been shown that electrical stimulation training enhances myofiber hypertrophy and metabolic flux.[79] Electrical stimulation training during 1 week of human myoblasts-derived muscle 3D bundles promoted an increase of myotube diameter by 40%. Using this electrical stimulation protocol, the authors measured the highest specific forces reported to date for an engineered human muscle (19.3 mN/mm^2). A more complex human skeletal muscle model was achieved by co-culturing primary human myoblasts with human stem cells-derived motoneurons in a fibrin-based hydrogel.[80] Briefly, Fibrin-Geltrex® hydrogels were fabricated by molding with Velcro® anchors that acted as artificial tendons to apply uniaxial tension. The resulting bioengineered human skeletal muscle tissues were able to form neuromuscular junctions (NMJs) in a long-lasting culture for up to 3 weeks (Figure 5(b)). NMJs play a key role in several muscular dystrophies,[88] which could be modeled following this innovative approximation.

3D bioprinting has also been applied to fabricate human skeletal muscle bundles.[81,83] Cell-laden fibrin bioink was bioprinted using gelatin as a sacrificial material to generate organized multilayered muscle bundles supported by a PCL pillar structure.[81] Myofibers in these bioartificial muscles were densely packed and highly aligned. The generated constructs were studied *in vivo*, where they achieved 82% of functional recovery in a rodent model of tibialis anterior muscle defect at 8 weeks of post-implantation. Good integration with host vascular and neural networks was observed. Alternatively, dECM have been used as a bioink for 3D printing of human skeletal muscle bundles.[83] Primary human myoblasts were printed with dECM from porcine muscular tissues in granule-based reservoirs. Moreover, coaxial printing with endothelial cells, using porcine blood vessel-derived dECM bioink, has allowed the prevascularization of these muscle bundles (Figure 5(c)). Implantation of these prevascularized muscle bundles in an injured muscle rodent model resulted in the high viability of the cells without generating hypoxia and enhanced *de novo* muscle formation.

Bioartificial muscles have been recently tested as drug screening platforms. Human myoblasts encapsulated in fibrin hydrogels were introduced in a device with a stereotactic setup that allows controllable injection at BAMs.[82] While most of the biological stimulation assays in 2D and 3D *in vitro* models are performed by adding a compound to the culture media, this setup allows modeling intramuscular drug delivery *in vitro*. Using spectrophotometry and luminescence, the release of the injected compounds and their metabolites were measured over time. Although these models are useful for intramuscular drug injection studies, their relatively large size limits their potential as a drug screening platform. BAMs fabrication requires large numbers of cells, which can be costly and difficult to obtain. Current microfabrication technologies have allowed the miniaturization of these tissues to obtain high-throughput systems.[46, 76, 89, 90] For example, a 96-well micro-muscle platform using primary human myoblasts.[76] Cells were encapsulated in a collagen-Matrigel® composite matrix around micropillars. The authors affirmed that with this approach, they could reduce the size, reagents, and cost by a factor of ≈25 compared to the state-of-the-art skeletal muscle bioengineering approaches mentioned above.[77,78] However, the reported specific forces and protein expression levels obtained with this miniaturized system are representative of immature muscle in a fetal-like state. Hence, intensive efforts in training and maturation of the micro-BAMs are needed to develop a successful high-throughput screening platform.

Modeling muscular dystrophies using tissue engineering

The intrinsic heterogeneity of muscular dystrophies means that the future of effective treatments for patients lies in personalized medicine. To date, mutations that cause specific muscular dystrophies have been described in more than 50 genes (Table 1). As a consequence of this genetic heterogeneity, specific muscle types are affected with a variable degree of progression in the dystrophic syndromes. Moreover, in some muscular dystrophies, disease progression and severity depend on individual patients. Therefore, developing *in vitro* bioengineered tissues in the laboratory from patient-derived cells is necessary to study personalized therapies. To date, much effort has been put

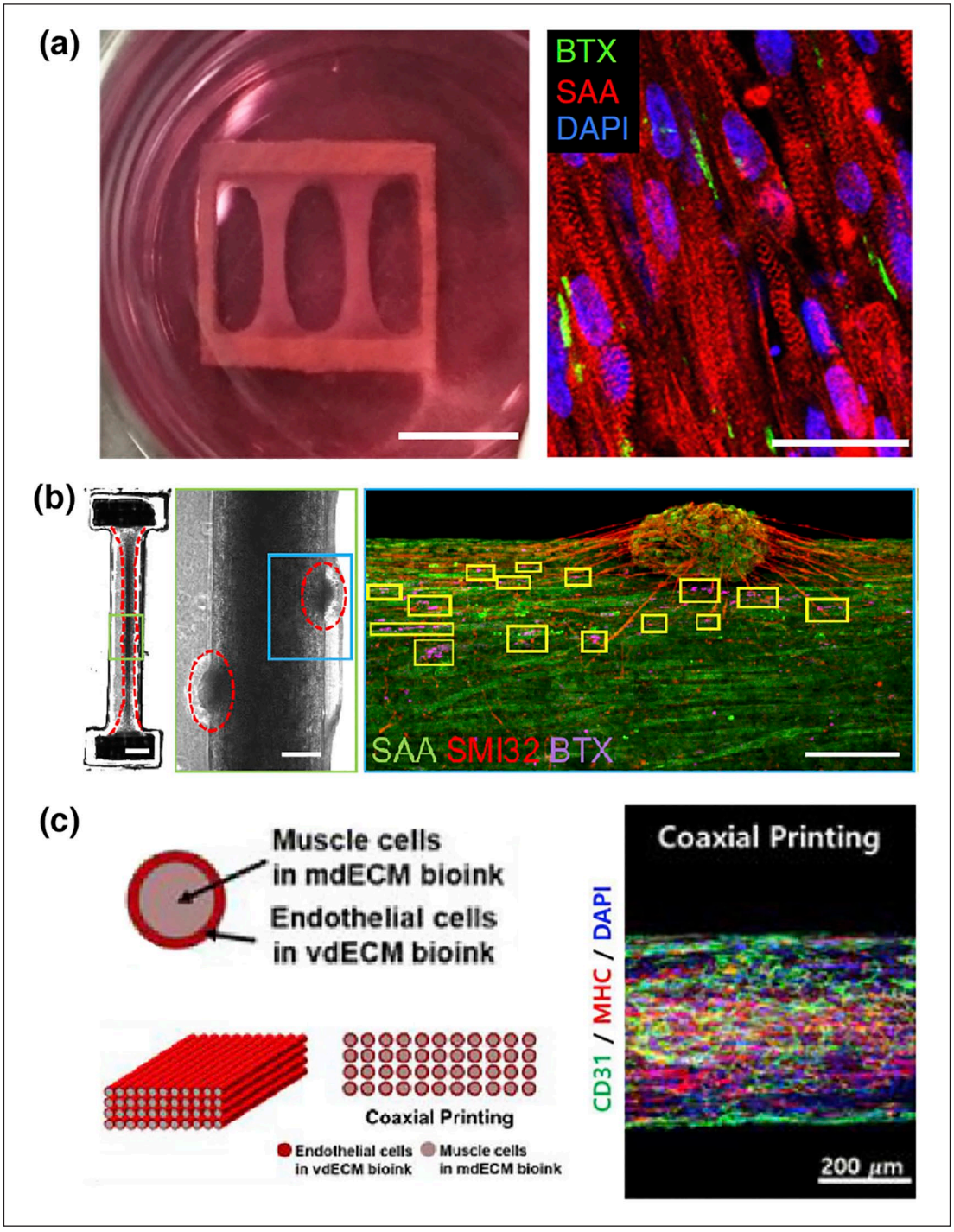

Figure 5. Human 3D engineered skeletal muscles. (a) Structure of hiPSC-derived muscle bundles anchored within a nylon frame. Scale bar: 5 mm. Representative longitudinal section of 2-week differentiated bundles showing aligned, cross-striated myotubes SAA = sarcomeric alpha-actinin, BTX = α-bungarotoxin labeling acetylcholine receptors (AChR) and DAPI counterstain myotube nuclei. Scale bar = 25 μm. Adapted from Rao et al.[78]. (b) Stitched phase contrast image of a representative 3D skeletal muscle-motor neuron (MN) co-culture. Neuromuscular tissue is outlined with a red dashed line in the left panel. The region outlined in the green box is magnified in the image to the immediate right. Red dashed lines in the right panel outline motoneuron clusters. Scale bars: 2 mm (left panel) and 200 mm (right panel). Adapted from Bakooshli et al.[80]. (c) Schematic representation of coaxial printing. Immunofluorescent image of a 3D printed muscle construct CD31 = cluster of differentiation 31 labeling endothelial cells, MHC = myosin heavy chain, and DAPI = stained nuclei. The images were taken from the center of the construct. Adapted with permission from Choi et al.[83]. The images in panel (c) are not published under the terms of the CC-BY license of this article. For permission to reuse, please see Choi et al.[83].

into developing better scaffolds or studying new biofabrication methods to develop skeletal muscle tissues *in vitro*. However, few works have introduced patient-derived cells, going a step further to create these personalized platforms. One of the first approximations was to culture myoblasts from Duchenne muscular dystrophy (DMD) patients on micropatterned polyacrylamide hydrogels functionalized with either laminin, fibronectin, or Matrigel®.[91] In this work, the authors functionalized the surface in parallel lines by micro-contact printing of these adhesion proteins. After 7 days of culture onto these hydrogels, the cells formed mature aligned myotubes with sarcomeric organization. Remarkably, myotubes cultured onto hydrogel with Matrigel® showed the highest level of expression of the muscle maturation markers as myosin heavy chain II and α-actinin. Moreover, DMD myotubes showed particular pathological hallmarks, such as the decreased expression of dystrophin, while the formation of sarcomeres remained unchanged. Although mature aligned myotubes could be obtained by culturing patient cells onto functionalized micropatterned polyacrylamide hydrogels, these 2D models do not represent the complexity of skeletal muscle tissues. In a recent study, human induced pluripotent stem cells (hiPSCs) were used to generate 3D engineered skeletal muscle tissues.[92] The authors cultivated human hiPSCs derived from Duchenne (DMD), limb-gridle, and other congenital muscular dystrophy patients encapsulated in fibrin hydrogels (Figure 6(a)). To mechanically stimulate myogenic differentiation, the hydrogels were cultured under tension. The resulting tissues showed mature myotube markers and recapitulated the pathogenic hallmarks of these muscular dystrophies. The authors investigate whether the 3D nature of the engineered skeletal muscle tissues would facilitate the detection of pathological hallmarks that are less evident in standard 2D cultures. To examine this, they generated artificial muscles from patient-derived hiPSC with muscular dystrophies caused by mutations in the LMNA gene. These diseases are also called laminopathies, and abnormalities in nuclear morphology are a key histological feature. LMNA mutant hiPSCs from patients with skeletal muscle laminopathies were used to create engineered skeletal muscle tissues, referred to by their mutation (i.e. LMNA L35P or LMNA R249W). Remarkably, 3D nuclear reconstruction of the engineered muscles highlighted features that were less prominent in traditional monolayer cultures. All mutant LMNA 3D engineered muscles showed a significant proportion of cells with nuclear aberrations (Figure 6(b)). These results demonstrate that these bioengineered skeletal muscle tissues from patient-derived cells are great tools to study the pathogenic pathways of muscular diseases and assay potential drugs. Nevertheless, the use of these platforms to test potential treatments for muscular dystrophies has not been reported yet. In 2009, Vandenburgh and colleagues developed an automated drug screening platform using contractile muscle tissue engineered from dystrophic myoblasts.[90] Primary myoblasts from the DMD mouse model (mdx mice) were encapsulated in a collagen-Matrigel® matrix and cast around two PDMS micro-pillars to engineer miniature bioartificial muscle (mBAMs).[46] These dystrophic mBAMs were electrically stimulated, and the force generation was measured. Then 31 drugs with potential anti-DMD effects were screened by measuring changes in force generation. Eleven drugs increased the dystrophic mBAMs tetanic force, similar to the response of DMD patients to many identical compounds. These results demonstrate the potential of this platform as a preclinical model. However, the use of mouse-derived cells is an important limitation of this approach since the heterogeneity of muscular dystrophy patients is not considered. Therefore, the integration of engineered skeletal muscle tissue from patient-derived cells in these automated drug screening platforms will bring powerful preclinical tools for these diseases.

Conclusions and perspectives

The latest advances in skeletal muscle tissue engineering have demonstrated the relevance of geometrical cues for the fabrication of *in vitro* muscle models. Aligned structures guide myotubes fusion and enhance the maturation of the myofibers.[37,39–42] Structured scaffolds can be obtained by bioprinting or molding biomaterials. Of note, the biomaterials for muscle engineering must provide mechanical support and allow nutrient diffusion through the scaffolds. Several studies conclude that electrical stimulation and mechanical tension favor the maturation of the tissues.[35,61,79] Current studies to develop human functional bioartificial muscle use fibrin-based hydrogels. Fibrin composite matrices have tunable mechanical properties, can be remodeled by cells, and allow long-term cultures.[78] The biomaterials developed to date successfully provide geometrical and mechanical cues for engineered skeletal muscle. In the native muscle, the ECM not only acts as a scaffold but is essential for cell signaling. Accordingly, the future biomaterials for skeletal muscle tissue engineering should combine physical and biochemical properties that better mimic the complexity of native ECM. Extensive works have developed new fabrication techniques and biomaterials compositions to obtain functional skeletal muscle tissues. Nevertheless, high maturation levels of myofibers have not yet been reached. Thus, the bioartificial tissues have not accurately modeled functional adult muscles. Several approaches have recently attempted to improve the maturation of the *in vitro* muscles, for example, implementing electrical stimulation training protocols and co-cultures.[79,80,83] Furthermore, incorporating endothelial cells to vascularize the tissues or innervation of the tissue with motoneurons are emerging strategies to obtain more complex skeletal muscle models. Innervation of

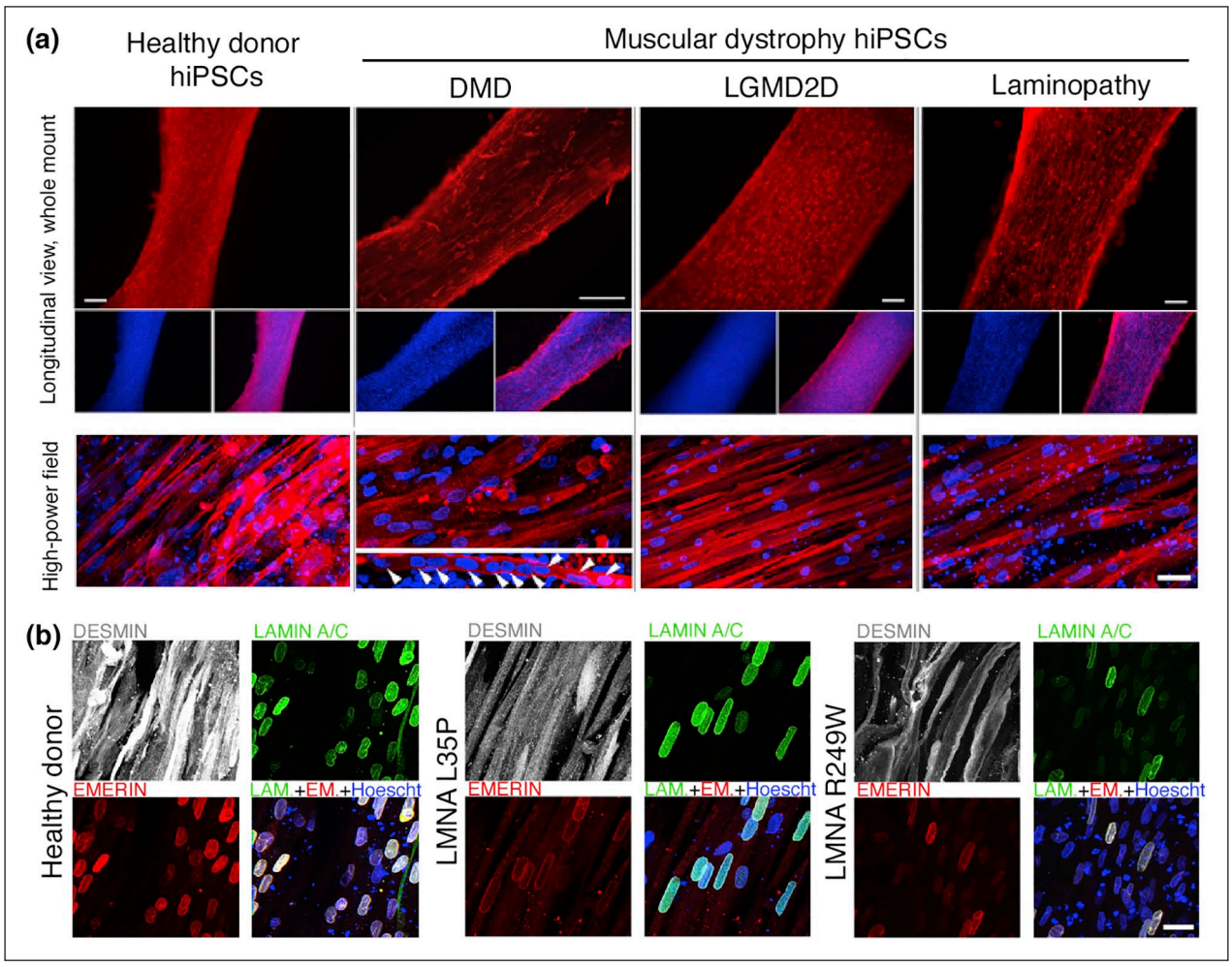

Figure 6. Modeling muscular dystrophies using tissue engineering. (a) 3D artificial skeletal muscle constructs derived from healthy and dystrophic hPSCs. Immunofluorescence for myosin heavy chain (MyHC) on muscle constructs derived from hESCs and dystrophic hiPSCs (DMD, LGMD2D, and skeletal muscle LMNA) differentiated in 3D for 10 days. Nuclei are counterstained with Hoechst. Arrowheads: multinucleated myotubes. Scale bars: top 250 μm, bottom 25 μm. (b) Confocal (z stacks merge) immunofluorescence for DESMIN (myotubes), LAMIN A/C, and EMERIN (nuclear lamina) on hiPSC-derived (healthy and LMNA mutant) artificial muscles. Hoechst: nuclei. Scale bars: 15 μm. Adapted from Maffioletti et al.[92].

muscle tissues with motoneurons is key for tissue maturation. Unfortunately, the protocols to obtain and co-culture motoneurons are complicated and not very well established. Hence, intensive research on co-culture techniques is one of the main future challenges. On the other hand, angiogenesis is still an important issue in tissue engineering. To date, full vascularization of engineered skeletal muscle tissue has not been achieved. Similar to motoneurons, it is essential to optimize protocols for co-culture. Besides, to mimic vascularized tissues, a specialized research field is focused on generating *in vitro* angiogenesis. The future perspective will be the confluence of both research areas to recreate the extensive network of blood capillaries in skeletal muscle.

Drug screening platforms exploiting new bioengineered skeletal muscle tissue models are promising tools to find treatments for muscular dystrophies. Interestingly, the integration of patient-derived cells to fabricate these bioartificial muscles could fill the gap in preclinical studies accelerating drug development. Moreover, patient-derived bioartificial muscles would allow testing personalized treatments *in vitro*, which are crucial due to the intrinsic heterogeneity of muscular dystrophy pathologies. Going a step further, these patient-derived bioartificial skeletal muscles can be integrated into microfluidic devices (organ-on-a-chip) with biosensors.[56,93,94] These microfluidic chips permit the precise control of drug administration. In addition, muscle metabolism and disease-specific markers could be analyzed in real-time. Classically, the outcomes of these drug experiments are measured at time series or end-points. The challenge in this technological field is to integrate new sensing platforms that obtain data during the assays in a non-destructive manner. Altogether, the studies reviewed in this article show that tissue engineering

technologies to develop these personalized drug screening platforms have a bright future perspective. Therefore, new efforts must point toward integrating patient-derived cells, biofabrication techniques, stimulation systems, and biosensors in personalized organ-on-a-chip preclinical platforms for muscular dystrophies.

Author contributions

JMF-C, XF-G, FV-M, and JR-A conceived this review. JMF-C coordinated the literature search and review design. JMF-C, XF-G, FV-M performed the literature search and wrote the paper. JMF-C generated the figures. JMF-C, XF-G, FV-M revised the manuscript and participated in the discussion with the input of JR-A.

Declaration of conflicting interests

The author(s) declared no potential conflicts of interest with respect to the research, authorship, and/or publication of this article.

Funding

The author(s) disclosed receipt of the following financial support for the research, authorship, and/or publication of this article: The authors acknowledge financial support from the European Research Council program under grants ERC-StG-DAMOC (714317), the Spanish Ministry of Economy and Competitiveness, through the "Severo Ochoa" Program for Centres of Excellence in R&D (SEV-2016-2019) and "Retos de investigación: proyectos I+D+i" (TEC2017-83716-C2-2-R), the CERCA Programme/Generalitat de Catalunya (2014-SGR-1460) and Fundación Bancaria "la Caixa"-Obra Social "la Caixa" (project IBEC-La Caixa Healthy Ageing) to JR-A. JMF-C was awarded with a postdoctoral fellowship (APOSTD/2017/088) from the Generalitat Valenciana, and XF-G was supported by a predoctoral fellowship (BES-2016-076681) from the Ministerio de Economia y Competitividad.

ORCID iDs

Juan M. Fernández-Costa https://orcid.org/0000-0002-1854-6082
Xiomara Fernández-Garibay https://orcid.org/0000-0002-0697-985X
Ferran Velasco-Mallorquí https://orcid.org/0000-0002-5681-800X
Javier Ramón-Azcón https://orcid.org/0000-0002-3636-8013

References

1. Mercuri E, Bönnemann CG and Muntoni F. Muscular dystrophies. *Lancet* 2019; 394: 2025–2038.
2. Benarroch L, Bonne G, Rivier F, et al. The 2020 version of the gene table of neuromuscular disorders (nuclear genome). *Neuromuscul Disord* 2019; 29: 980–1018.
3. Carter JC, Sheehan DW, Prochoroff A, et al. Muscular dystrophies. *Clin Chest Med* 2018; 39: 377–389.
4. Vydra DG and Rayi A. *Myotonic dystrophy*. Treasure Island: StatPearls Publishing, 2020.
5. Yiu EM and Kornberg AJ. Duchenne muscular dystrophy. *J Paediatr Child Health* 2015; 51: 759–764.
6. Mah JK, Korngut L, Fiest KM, et al. A systematic review and meta-analysis on the epidemiology of the muscular dystrophies. *Can J Neurol Sci/J Can des Sci Neurol* 2016; 43: 163–177.
7. Verhaart IEC and Aartsma-Rus A. Therapeutic developments for Duchenne muscular dystrophy. *Nat Rev Neurol* 2019; 15: 373–386.
8. Datta N and Ghosh PS. Update on muscular dystrophies with focus on novel treatments and biomarkers. *Curr Neurol Neurosci Rep* 2020; 20: 14.
9. López Castel A, Overby SJ and Artero R. MicroRNA-based therapeutic perspectives in myotonic dystrophy. *Int J Mol Sci* 2019; 20: 5600.
10. Reddy K, Jenquin JR, Cleary JD, et al. Mitigating RNA toxicity in myotonic dystrophy using small molecules. *Int J Mol Sci* 2019; 20: 4017.
11. Overby SJ, Cerro-Herreros E, Llamusi B, et al. RNA-mediated therapies in myotonic dystrophy. *Drug Discov Today* 2018; 23: 2013–2022.
12. Wouters OJ, McKee M and Luyten J. Estimated research and development investment needed to bring a new medicine to market, 2009–2018. *JAMA* 2020; 323: 844–853.
13. Dowden H and Munro J. Trends in clinical success rates and therapeutic focus. *Nat Rev Drug Discov* 2019; 18: 495–496.
14. Kankala RK, Wang S-B and Chen A-Z. Microengineered organ-on-a-chip platforms towards personalized medicine. *Curr Pharm Des* 2019; 24: 5354–5366.
15. Martinez E, St-Pierre J-P and Variola F. Advanced bioengineering technologies for preclinical research. *Adv Phys X* 2019; 4: 1622451.
16. Frontera WR and Ochala J. Skeletal muscle: a brief review of structure and function. *Calcif Tissue Int* 2015; 96: 183–195.
17. Chal J and Pourquié O. Making muscle: skeletal myogenesis in vivo and in vitro. *Development* 2017; 144: 2104–2122.
18. Mukund K and Subramaniam S. Skeletal muscle: a review of molecular structure and function, in health and disease. *Wiley Interdiscip Rev Syst Biol Med* 2020; 12: e1462.
19. Zammit PS. Function of the myogenic regulatory factors Myf5, MyoD, myogenin and MRF4 in skeletal muscle, satellite cells and regenerative myogenesis. *Semin Cell Dev Biol* 2017; 72: 19–32.
20. Yin H, Price F and Rudnicki MA. Satellite cells and the muscle stem cell niche. *Physiol Rev* 2013; 93: 23–67.
21. Buckingham M. Skeletal muscle progenitor cells and the role of Pax genes. *C R Biol* 2007; 330: 530–533.
22. Sanger JW, Chowrashi P, Shaner NC, et al. Myofibrillogenesis in skeletal muscle cells. *Clin Orthop Relat Res* 2002; 403: S153–S162.
23. Csapo R, Gumpenberger M and Wessner B. Skeletal muscle extracellular matrix – what do we know about its composition, regulation, and physiological roles? A narrative review. *Front Physiol* 2020; 11: 1–15.
24. Gillies AR and Lieber RL. Structure and function of the skeletal muscle extracellular matrix. *Muscle Nerve* 2011; 44: 318–331.
25. Hinds S, Bian W, Dennis RG, et al. The role of extracellular matrix composition in structure and function of bioengineered skeletal muscle. *Biomaterials* 2011; 32: 3575–3583.
26. Bushby KMD, Collins J and Hicks D. Collagen type VI myopathies. In: Halper J (ed.) *Progress in heritable soft*

connective tissue diseases. Dordrecht, Netherlands: Springer, pp.185–199.
27. Denes LT, Riley LA, Mijares JR, et al. Culturing C2C12 myotubes on micromolded gelatin hydrogels accelerates myotube maturation. *Skelet Muscle* 2019; 9: 17.
28. Vajanthri KY, Sidu RK and Mahto SK. Micropatterning and alignment of skeletal muscle myoblasts using microflowed plasma process. *Irbm* 2020; 41: 48–57.
29. Kim J, Leem J, Kim HN, et al. Uniaxially crumpled graphene as a platform for guided myotube formation. *Microsyst Nanoeng* 2019; 5: 53.
30. Park J, Choi JH, Kim S, et al. Micropatterned conductive hydrogels as multifunctional muscle-mimicking biomaterials: Graphene-incorporated hydrogels directly patterned with femtosecond laser ablation. *Acta Biomater* 2019; 97: 141–153.
31. Gong HY, Park J, Kim W, et al. A novel conductive and micropatterned PEG-based hydrogel enabling the topographical and electrical stimulation of myoblasts. *ACS Appl Mater Interfaces* 2019; 11: 47695–47706.
32. Xue J, Wu T, Dai Y, et al. Electrospinning and electrospun nanofibers: methods, materials, and applications. *Chem Rev* 2019; 119: 5298–5415.
33. Somers SM, Zhang NY, Morrissette-McAlmon JBF, et al. Myoblast maturity on aligned microfiber bundles at the onset of strain application impacts myogenic outcomes. *Acta Biomater* 2019; 94: 232–242.
34. Yeo M and Kim GH. Micro/nano-hierarchical scaffold fabricated using a cell electrospinning/3D printing process for co-culturing myoblasts and HUVECs to induce myoblast alignment and differentiation. *Acta Biomater* 2020; 107: 102–114.
35. Ribeiro S, Gomes AC, Etxebarria I, et al. Electroactive biomaterial surface engineering effects on muscle cells differentiation. *Mater Sci Eng C* 2018; 92: 868–874.
36. Ribeiro C, Sencadas V, Correia DM, et al. Piezoelectric polymers as biomaterials for tissue engineering applications. *Colloids Surf B Biointerfaces* 2015; 136: 46–55.
37. Kim J, Kim W and Kim G. Scaffold with micro/nanoscale topographical cues fabricated using E-field-assisted 3D printing combined with plasma-etching for enhancing myoblast alignment and differentiation. *Appl Surf Sci* 2020; 509: 145404.
38. Du W, Hong S, Scapin G, et al. Directed collective cell migration using three-dimensional bioprinted micropatterns on thermoresponsive surfaces for myotube formation. *ACS Biomater Sci Eng* 2019; 5: 3935–3943.
39. Shi X, Ostrovidov S, Zhao Y, et al. Microfluidic spinning of cell-responsive grooved microfibers. *Adv Funct Mater* 2015; 25: 2250–2259.
40. Ebrahimi M, Ostrovidov S, Salehi S, et al. Enhanced skeletal muscle formation on microfluidic spun gelatin methacryloyl (GelMA) fibres using surface patterning and agrin treatment. *J Tissue Eng Regen Med* 2018; 12: 2151–2163.
41. Nakayama KH, Quarta M, Paine P, et al. Treatment of volumetric muscle loss in mice using nanofibrillar scaffolds enhances vascular organization and integration. *Commun Biol* 2019; 2: 170.
42. Lai ES, Huang NF, Cooke JP, et al. Aligned nanofibrillar collagen regulates endothelial organization and migration. *Regen Med* 2012; 7: 649–661.
43. Ostrovidov S, Salehi S, Costantini M, et al. 3D Bioprinting in skeletal muscle tissue engineering. *Small* 2019; 15: 1–14.
44. Seyedmahmoud R, Çelebi-Saltik B, Barros N, et al. Three-dimensional bioprinting of functional skeletal muscle tissue using gelatinmethacryloyl-alginate bioinks. *Micromachines* 2019; 10: 679.
45. Mestre R, Patiño T, Barceló X, et al. Force modulation and adaptability of 3D-bioprinted biological actuators based on skeletal muscle tissue. *Adv Mater Technol* 2019; 4: 1800631.
46. Vandenburgh H, Shansky J, Benesch-Lee F, et al. Drug-screening platform based on the contractility of tissue-engineered muscle. *Muscle Nerve* 2008; 37: 438–447.
47. Distler T, Solisito AA, Schneidereit D, et al. 3D printed oxidized alginate-gelatin bioink provides guidance for C2C12 muscle precursor cell orientation and differentiation via shear stress during bioprinting. *Biofabrication* 2020; 12: 045005.
48. Kim WJ and Kim GH. 3D bioprinting of functional cell-laden bioinks and its application for cell-alignment and maturation. *Appl Mater Today* 2020; 19: 100588.
49. Kim WJ, Jang CH and Kim GH. A Myoblast-laden collagen bioink with fully aligned Au nanowires for muscle-tissue regeneration. *Nano Lett* 2019; 19: 8612–8620.
50. García-Lizarribar A, Fernández-Garibay X, Velasco-Mallorquí F, et al. Composite biomaterials as long-lasting scaffolds for 3D bioprinting of highly aligned muscle tissue. *Macromol Biosci* 2018; 18: 1800167.
51. Costantini M, Testa S, Mozetic P, et al. Microfluidic-enhanced 3D bioprinting of aligned myoblast-laden hydrogels leads to functionally organized myofibers in vitro and in vivo. *Biomaterials* 2017; 131: 98–110.
52. Mozetic P, Giannitelli SM, Gori M, et al. Engineering muscle cell alignment through 3D bioprinting. *J Biomed Mater Res—Pt A* 2017; 105: 2582–2588.
53. Chen H, Zhong J, Wang J, et al. Enhanced growth and differentiation of myoblast cells grown on E-jet 3D printed platforms. *Int J Nanomedicine* 2019; 14: 937–950.
54. Kalman B, Monge C, Bigot A, et al. Engineering human 3D micromuscles with co-culture of fibroblasts and myoblasts. *Comput Methods Biomech Biomed Eng* 2015; 5842: 1–2.
55. Costantini M, Testa S, Fornetti E, et al. Engineering muscle networks in 3D gelatin methacryloyl hydrogels: influence of mechanical stiffness and geometrical confinement. *Front Bioeng Biotechnol* 2017; 5: 1–8.
56. Ortega MA, Fernández-Garibay X, Castaño AG, et al. Muscle-on-a-chip with an on-site multiplexed biosensing system for: in situ monitoring of secreted IL-6 and TNF-α. *Lab Chip* 2019; 19: 2568–2580.
57. Hernández-Albors A, Castaño AG, Fernández-Garibay X, et al. Microphysiological sensing platform for an in-situ detection of tissue-secreted cytokines. *Biosens Bioelectron X* 2019; 2: 100025.
58. Wan L, Flegle J, Ozdoganlar B, et al. Toward vasculature in skeletal muscle-on-a-chip through thermo-responsive sacrificial templates. *Micromachines* 2020; 11: 907.
59. Christensen RK, Von Halling Laier C, Kiziltay A, et al. 3D printed hydrogel multiassay platforms for robust generation of engineered contractile tissues. *Biomacromolecules* 2020; 21: 356–365.

60. Singh D, Nayak V and Kumar A. Proliferation of myoblast skeletal cells on three-dimensional supermacroporous cryogels. *Int J Biol Sci* 2010; 6: 371–381.
61. Velasco-Mallorquí F, Fernández-Costa JM, Neves L, et al. New volumetric CNT-doped gelatin–cellulose scaffolds for skeletal muscle tissue engineering. *Nanoscale Adv* 2020; 2: 2885–2896.
62. Kankala RK, Zhao J, Liu CG, et al. Highly porous microcarriers for minimally invasive in situ skeletal muscle cell delivery. *Small* 2019; 15: 1–15.
63. Bettadapur A, Suh GC, Geisse NA, et al. Prolonged culture of aligned skeletal myotubes on micromolded gelatin hydrogels. *Sci Rep* 2016; 6: 1–14.
64. Tanaka N, Ota H, Fukumori K, et al. Micro-patterned cell-sheets fabricated with stamping-force-controlled microcontact printing. *Biomaterials* 2014; 35: 9802–9810.
65. Lee H, Ju YM, Kim I, et al. A novel decellularized skeletal muscle-derived ECM scaffolding system for in situ muscle regeneration. *Methods* 2020; 171: 77–85.
66. Kim W, Lee H, Lee J, et al. Efficient myotube formation in 3D bioprinted tissue construct by biochemical and topographical cues. *Biomaterials* 2020; 230: 119632.
67. Badylak SF, Freytes DO and Gilbert TW. Extracellular matrix as a biological scaffold material: structure and function. *Acta Biomater* 2009; 5: 1–13.
68. Béduer A, Braschler T, Peric O, et al. A compressible scaffold for minimally invasive delivery of large intact neuronal networks. *Adv Healthc Mater* 2015; 4: 301–312.
69. Wu X, Liu Y, Li X, et al. Preparation of aligned porous gelatin scaffolds by unidirectional freeze-drying method. *Acta Biomater* 2010; 6: 1167–1177.
70. Wu J, Zhao Q, Sun J, et al. Preparation of poly(ethylene glycol) aligned porous cryogels using a unidirectional freezing technique. *Soft Matter* 2012; 8: 3620.
71. Torii R, Velliou R-I, Hodgson D, et al. Modelling multiscale cell–tissue interaction of tissue-engineered muscle constructs. *J Tissue Eng* 2018; 9: 204173141878714.
72. Smith AST, Passey S, Greensmith L, et al. Characterization and optimization of a simple, repeatable system for the long term in vitro culture of aligned myotubes in 3D. *J Cell Biochem* 2012; 113: 1044–1053.
73. Wang J, Khodabukus A, Rao L, et al. Engineered skeletal muscles for disease modeling and drug discovery. *Biomaterials* 2019; 221: 119416.
74. Zhang D, Yan K, Zhou J, et al. Myogenic differentiation of human amniotic mesenchymal cells and its tissue repair capacity on volumetric muscle loss. *J Tissue Eng* 2019; 10: 204173141988710.
75. Powell CA, Smiley BL, Mills J, et al. Mechanical stimulation improves tissue-engineered human skeletal muscle. *Am J Physiol Cell Physiol* 2002; 283: 1557–1565.
76. Mills RJ, Parker BL, Monnot P, et al. Development of a human skeletal micro muscle platform with pacing capabilities. *Biomaterials* 2019; 198: 217–227.
77. Madden L, Juhas M, Kraus WE, et al. Bioengineered human myobundles mimic clinical responses of skeletal muscle to drugs. *Elife* 2015; 2015: 1–14.
78. Rao L, Qian Y, Khodabukus A, et al. Engineering human pluripotent stem cells into a functional skeletal muscle tissue. *Nat Commun* 2018; 9: 126.
79. Khodabukus A, Madden L, Prabhu NK, et al. Electrical stimulation increases hypertrophy and metabolic flux in tissue-engineered human skeletal muscle. *Biomaterials* 2019; 198: 259–269.
80. Bakooshli MA, Lippmann ES, Mulcahy B, et al. A 3D culture model of innervated human skeletal muscle enables studies of the adult neuromuscular junction. *Elife* 2019; 8: 1–29.
81. Kim JH, Seol YJ, Ko IK, et al. 3D bioprinted human skeletal muscle constructs for muscle function restoration. *Sci Rep* 2018; 8: 1–15.
82. Gholobova D, Gerard M, Decroix L, et al. Human tissue-engineered skeletal muscle: a novel 3D in vitro model for drug disposition and toxicity after intramuscular injection. *Sci Rep* 2018; 8: 1–14.
83. Choi Y-J, Jun Y-J, Kim DY, et al. A 3D cell printed muscle construct with tissue-derived bioink for the treatment of volumetric muscle loss. *Biomaterials* 2019; 206: 160–169.
84. Okano T and Matsuda T. Tissue engineered skeletal muscle: preparation of highly dense, highly oriented hybrid muscular tissues. *Cell Transplant* 1998; 7: 71–82.
85. Vandenburgh HH, Karlisch P and Farr L. Maintenance of highly contractile tissue-cultured avian skeletal myotubes in collagen gel. *Vitr Cell Dev Biol* 1988; 24: 166–174.
86. Khodabukus A and Baar K. Factors that affect tissue-engineered skeletal muscle function and physiology. *Cells Tissues Organs* 2016; 202: 159–168.
87. Chiron S, Tomczak C, Duperray A, et al. Complex interactions between human myoblasts and the surrounding 3D fibrin-based matrix. *PLoS One* 2012; 7: 2–9.
88. Rudolf R, Khan MM, Labeit S, et al. Degeneration of neuromuscular junction in age and dystrophy. *Front Aging Neurosci* 2014; 6: 99.
89. Ramade A, Legant WR, Picart C, et al. Microfabrication of a platform to measure and manipulate the mechanics of engineered microtissues. In: *Methods in cell biology*. London: Elsevier Inc., pp.191–211.
90. Vandenburgh H, Shansky J, Benesch-Lee F, et al. Automated drug screening with contractile muscle tissue engineered from dystrophic myoblasts. *FASEB J* 2009; 23: 3325–3334.
91. Serena E, Zatti S, Reghelin E, et al. Soft substrates drive optimal differentiation of human healthy and dystrophic myotubes. *Integr Biol (Camb)* 2010; 2: 193–201.
92. Maffioletti SM, Sarcar S, Henderson ABH, et al. Three-dimensional human iPSC-derived artificial skeletal muscles model muscular dystrophies and enable multilineage tissue engineering. *Cell Rep* 2018; 23: 899–908.
93. Agrawal G, Aung A and Varghese S. Skeletal muscle-on-a-chip: an in vitro model to evaluate tissue formation and injury. *Lab Chip* 2017; 17: 3447–3461.
94. Osaki T, Uzel SGM and Kamm RD. On-chip 3D neuromuscular model for drug screening and precision medicine in neuromuscular disease. *Nat Protoc* 2020; 15: 421–449.